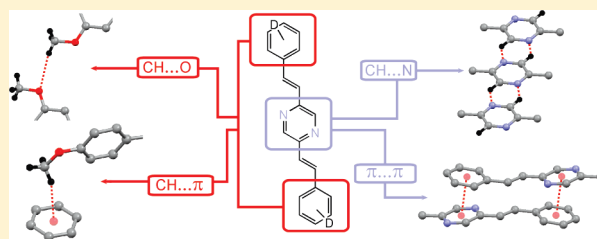


Competition between Methoxy-Based and Pyrazine-Based Synthons in Methoxy-Substituted Distyrylpyrazines

Alain Collas,[†] Izabela Bagrowska,[‡] Krzysztof Aleksandrak,[‡] Matthias Zeller,[§] and Frank Blockhuys^{*,†}[†]Department of Chemistry, University of Antwerp, Universiteitsplein 1, B-2610 Antwerp, Belgium[‡]Faculty of Chemistry, Nicolaus Copernicus University, Gagarina 7, PL-87100 Toruń, Poland[§]Department of Chemistry, Youngstown State University, One University Plaza, Youngstown, Ohio 44555-3663, United States

S Supporting Information

ABSTRACT: Four new methoxy-substituted derivatives of *E,E*-2,5-bis(2-phenylethenyl)pyrazine have been synthesized. The supramolecular structures of the resulting set of five polymorphs have been studied using single-crystal X-ray diffraction to gauge the influence of the position of the methoxy groups on the organization of the molecules in the solid state, as part of an attempt to dispense with the particular polymorphism of the parent compound. The crystal packing patterns were analyzed in terms of the two pyrazine-based synthons found in the parent compound's crystal structure, the $\pi_{\text{pyrazine}} \cdots \pi_{\text{phenyl}}$ stacking synthon, and the pyrazine hydrogen-bonded synthon, as well as in terms of weak intermolecular interactions such as $\text{CH} \cdots \text{O}$, $\text{CH} \cdots \text{N}$, and $\text{CH} \cdots \pi$. The analysis shows that the introduction of methoxy groups in positions other than only the para position of the peripheral benzene rings successfully switches off the two synthons seen in the parent compound and that the new compounds adopt other packing strategies, based on methoxy \cdots methoxy and $-\text{OCH}_3 \cdots \pi$ contacts. Polymorphism, however, remains.



1. INTRODUCTION

Organic semiconductors of the distyrylbenzene type (DSB), oligomers of poly(*p*-phenylene vinylene) (PPV), have great potential as active materials in opto-electronic devices in which they can be used, among others, for the construction of organic light-emitting devices (OLEDs)^{1–5} and as memory and non-linear optical (NLO) materials.^{6,7} To improve their relevant properties, such as the efficiency of light emission for OLED materials, a number of molecular engineering strategies have been developed. One of these is to lower the barrier to electron injection by increasing the electron affinity of the material. This can be achieved by substituting the DSB backbone with electron-withdrawing groups, but since such operations are very often accompanied by a decrease in solubility and volatility, which severely hampers device construction, a more convenient strategy is to integrate electron-withdrawing heteroatoms into the DSB backbone. This incorporation strategy has been successfully applied by Nohara et al.⁸ and Grimsdale et al.⁹ resulting in a dimethoxy derivative of *E,E*-2,5-bis(2-phenylethenyl)pyrazine (**1**, Figure 1), that is, *E,E*-2,5-bis[2-(4-methoxyphenyl)ethenyl]pyrazine (**2**), which indeed displays a higher electron affinity than PPV.

Even though the favorable molecular properties of these nitrogen-containing DSBs have been demonstrated, it is clear that using these materials in the above-mentioned applications means that not only the molecular but also the supramolecular aspect is of importance and that a detailed knowledge of the

solid-state structure of the compounds is indispensable. However, until today no systematic study has been conducted: the only two distyrylpyrazines (DSPs) of which structures have been reported are the parent compound (**1**)^{10,11} and **2**,¹² and in each case two polymorphs were reported.

Even though from a structural chemistry point of view the presence of polymorphism may be seen as advantageous, since it provides an opportunity to study and understand the nature of the interactions influencing a molecule during crystal packing, it is clear that from a materials chemistry point of view it is not: the fact that **1** and **2** suffer from polymorphism holds a number of serious repercussions in particular for the construction and evaluation of the above-mentioned devices. Conclusions with respect to, for example, the efficiency of light emission or mechanistic aspects, drawn from the results of electrical and optical measurements, may be erroneous as **1** can exist in a form (its α -form) that is capable of undergoing a solid-state photopolymerization. Indeed, the noncovalent interactions between the aromatic moieties, which will be discussed below in greater detail, help to establish the typical face-to-face stacking (Figure 2a) and, in this way, to meet the conditions to undergo a cycloaddition reaction: when the ethenyl spacers are separated

Received: November 16, 2010

Revised: January 17, 2011

Published: February 10, 2011

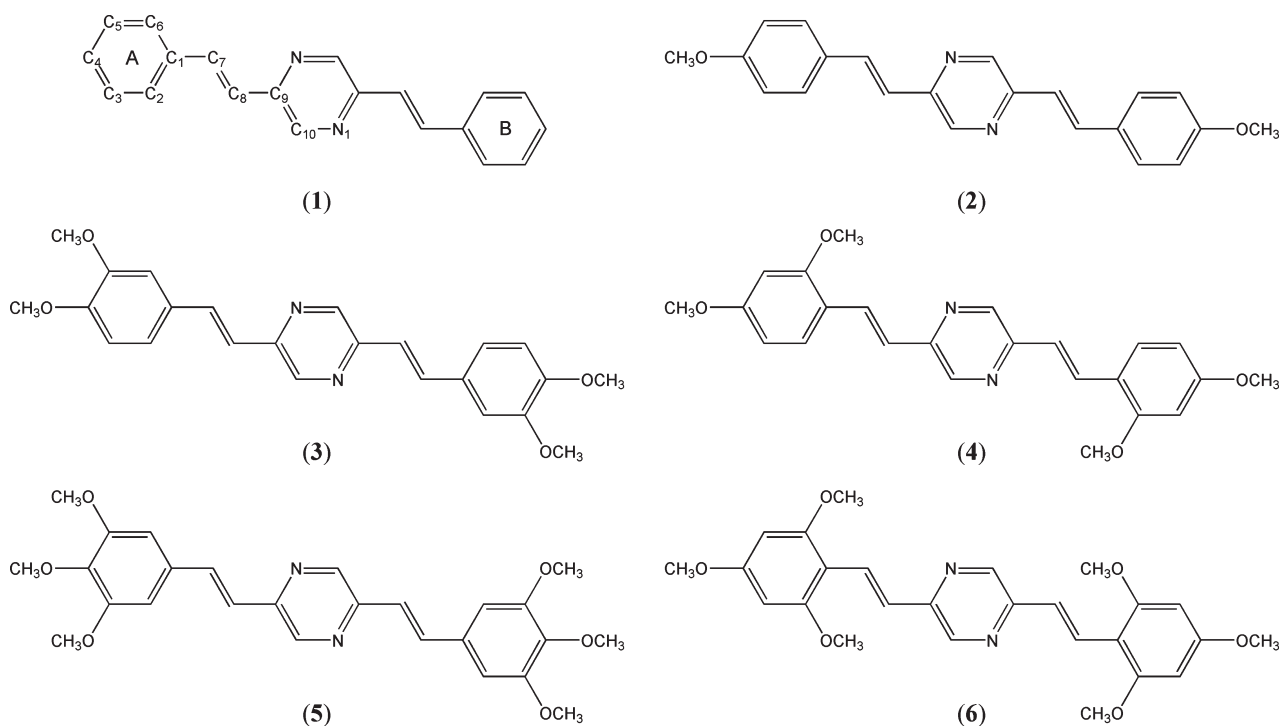


Figure 1. The parent DSP (**1**) and its five methoxy-substituted derivatives (**2–6**). The structural formula of **1** presents the numbering scheme of the five compounds; in polymorph **1a** the molecules have no inversion symmetry and the numbering in the second half of the molecule (containing ring B) mirrors the numbering in the first (containing ring A) with a suffix D added to the atom label.

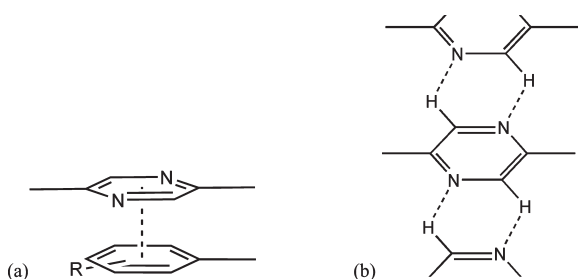


Figure 2. (a) The $\pi_{\text{pyrazine}} \cdots \pi_{\text{phenyl}}$ stacking synthon and (b) the pyrazine hydrogen-bonded synthon.

by less than 4.2 Å, these crystals yield, after irradiation with UV-light with an appropriate wavelength, photoproducts with a well-defined yet altered stereochemical and supramolecular structure;¹³ the photo-oligomerization and -polymerization of **1** have been studied in detail.¹⁴ In contrast, the second modification of **1** (its γ -form) is photostable. Compound **2** displays similar polymorphism as it too has a modification that is capable of undergoing a solid-state photopolymerization (its α -form), as well as a photostable modification (its γ -form). The former also displays the $\pi_{\text{pyrazine}} \cdots \pi_{\text{phenyl}}$ synthon (Figure 2a). Both the photostable modifications of **1** and **2**, on the other hand, display the typical pyrazine hydrogen-bonded synthon (Figure 2b). The fact that both compounds in this series are found in the same types of polymorphs suggests that both synthons presented in Figure 2 have a similar stabilizing effect on the supramolecular structure, despite the fact that they are based on different weak interactions.

In an attempt to deal with this unfortunate polymorphism in order to take full advantage of the compounds' molecular properties, a series of new DSPs were prepared and characterized containing two or three methoxy groups per peripheral ring,

since it is clear from the fact that **1** and **2** display similar polymorphism that one methoxy group positioned para on each of the peripheral rings is incapable of having a large enough effect. These compounds are *E,E*-2,5-bis[2-(3,4-dimethoxyphenyl)ethenyl]pyrazine (**3**), *E,E*-2,5-bis[2-(2,4-dimethoxyphenyl)ethenyl]pyrazine (**4**), *E,E*-2,5-bis[2-(3,4,5-trimethoxyphenyl)ethenyl]pyrazine (**5**), and *E,E*-2,5-bis[2-(2,4,6-trimethoxyphenyl)ethenyl]pyrazine (**6**); their structural formulas are shown in Figure 1. The introduction of these substituents results in the exploitation of two effects. First, the extra methoxy groups on the peripheral rings necessarily increase the intermolecular distance between the molecules in the solid, leading to the switching off of the typical pyrazine hydrogen-bonded synthon (Figure 2b) seen in the photostable γ -forms of **1** and **2**. Second, methoxy groups tend to favor reciprocal contacts among each other: this has been demonstrated in our previous work on methoxy-substituted distyrylbenzenes,^{15,16} but it can also be seen clearly in the solid-state structure of both polymorphs of **2** (see below). Because of these favored methoxy \cdots methoxy contacts $\pi \cdots \pi$ stacking becomes increasingly unlikely, thereby also switching off the $\pi_{\text{pyrazine}} \cdots \pi_{\text{phenyl}}$ synthon (Figure 2a). These two effects are expected to lead to the disappearance of the polymorphs observed for **1** and **2** and force the molecules of the new compounds into a different supramolecular organization.

2. EXPERIMENTAL SECTION

2.1. Syntheses. All reagents and solvents were obtained from ACROS and used as received. All NMR spectra were recorded in CDCl_3 on a Bruker Avance II spectrometer at frequencies of 400 MHz for ^1H and 100 MHz for ^{13}C with tetramethylsilane (TMS) as internal standard. Chemical shifts are given in ppm and coupling constants are in Hz. UV/vis absorption spectra were recorded on a Cary 5 spectrometer for solutions

(about 20×10^{-6} M) of the oligomers in CH_2Cl_2 . Melting points were obtained with an open capillary electrothermal melting point apparatus and are uncorrected. Preparative details and spectroscopic characterization of compounds **2** and **4** can be found in the Supporting Information.

2.1.1. *E,E*-2,5-Bis[2-(3,4-dimethoxyphenyl)ethenyl]pyrazine (3). A round-bottomed flask was charged with 4.2 g (25 mmol) of 3,4-dimethoxybenzaldehyde and 1.4 g (12.5 mmol) of 2,5-dimethylpyrazine in 20 mL of DMF. After 30 min, 2.8 g (50 mmol) of KOH was added. The mixture was heated to 100 °C and stirred at this temperature for 4 days. After cooling to room temperature, the mixture was cooled in an ice bath and 60 mL of cold methanol was added. The mixture was stored overnight in the refrigerator and the resulting orange precipitate was washed with water (2×20 mL) and ethanol (2×20 mL). The crude product was isomerized for 4 h in refluxing *p*-xylene containing a catalytic amount of I_2 . The precipitate was collected by filtration and washed with water (2×20 mL) and ethanol (2×20 mL) and recrystallized from a 5:1 mixture of ethanol and propanol. The yield was 5.8%. Mp 502 (polymorph **3a**), 487 K (polymorph **3b**). UV/vis $\lambda_{\text{max}} = 410$ nm ($\log \epsilon = 4.74$). $\delta^1\text{H}$ 3.93 (s, 6H, 4-OCH₃), 3.96 (s, 6H, 3-OCH₃), 6.89 (d, $J = 8.8$ Hz, 2H, H5), 7.04 (d, $J = 16.0$ Hz, 2H, H8), 7.16 (m, 4H, H2 and H6), 7.67 (d, $J = 16.0$, 2H, H7), 8.57 (s, 2H, H10). $\delta^{13}\text{C}$ 55.91 (4-OCH₃), 55.97 (3-OCH₃), 109.24 (C2), 111.28 (C5), 121.21 (C6), 122.26 (C8), 129.47 (C1), 133.91 (C7), 142.94 (C10), 149.01 (C4), 149.28 (C3), 150.01 (C9). Crystals of **3a** and **3b** suitable for a diffraction experiment were crystallized concomitantly via the slow evaporation of an acetone solution and separated manually under a microscope.

2.1.2. *E,E*-2,5-Bis[2-(3,4,5-trimethoxyphenyl)ethenyl]pyrazine (5). A round-bottomed flask was charged with 4.9 g (25 mmol) of 3,4,5-trimethoxybenzaldehyde and 1.4 g (12.5 mmol) of 2,5-dimethylpyrazine in 30 mL of DMF. After 30 min, 2.8 g (50 mmol) of KOH was added. The mixture was heated to 100 °C and stirred at this temperature for 6 days. After cooling to room temperature, the mixture was cooled in an ice bath and 70 mL of cold methanol was added. The mixture was stored overnight in the refrigerator and the resulting orange precipitate was washed with water (2×20 mL) and ethanol (2×20 mL). The crude product was isomerized for 4 h in refluxing *p*-xylene containing a catalytic amount of I_2 . The precipitate was collected by filtration and washed with water (2×20 mL) and ethanol (2×20 mL) and recrystallized from acetonitrile. The yield was 3.7%. Mp 484 (polymorph **5a**), 490 K (polymorph **5b**). UV/vis $\lambda_{\text{max}} = 402$ nm ($\log \epsilon = 4.63$). $\delta^1\text{H}$ 3.90 (s, 6H, 3-OCH₃), 3.92 (s, 12H, 3-OCH₃ and 5-OCH₃), 6.84 (s, 4H, H2, and H6), 7.09 (d, $J = 16.00$, 2H, H8), 7.66 (d, $J = 16.00$, 2H, H7), 8.60 (s, 2H, H10). $\delta^{13}\text{C}$ 56.16 (3-OCH₃ and 5-OCH₃), 61.00 (4-OCH₃), 104.40 (C2 and C6), 123.51 (C8), 131.89 (C1), 134.27 (C7), 139.05 (C4), 143.13 (C10), 148.96 (C3 and C5), 153.49 (C9). Crystals suitable for a diffraction experiment were grown by introducing small needle-shaped crystals obtained from a sublimation experiment into a saturated CHCl_3 solution. Slow evaporation of this solution yielded larger, suitable needle-shaped crystals of polymorph **5a**. A small amount of block-shaped crystals (polymorph **5b**) was found in the same batch and was used in the measurement. Since that time, however, we have been unable to obtain more crystals of polymorph **5b**.

2.1.3. *E,E*-2,5-Bis[2-(2,4,6-trimethoxyphenyl)ethenyl]pyrazine (6). A round-bottomed flask was charged with 4.9 g (25 mmol) of 2,4,6-trimethoxybenzaldehyde and 1.4 g (12.5 mmol) of 2,5-dimethylpyrazine in 30 mL of DMF. After 30 min, 2.8 g (50 mmol) of KOH was added. The mixture was heated to 100 °C and stirred at this temperature for 7 days. After cooling to room temperature, the mixture was cooled in an ice bath and 90 mL of cold methanol was added. The mixture was stored overnight in the refrigerator and the resulting orange precipitate was washed with water (2×20 mL) and ethanol (2×20 mL). The crude product was isomerized for 4 h in refluxing *p*-xylene containing a catalytic amount of I_2 . The precipitate was collected by filtration and washed with water (2×20 mL) and ethanol (2×20 mL) and recrystallized from a 5:2

mixture of acetonitrile and chloroform. The yield was 3.5%. Mp > 523 K. UV/vis $\lambda_{\text{max}} = 419$ nm ($\log \epsilon = 4.65$). $\delta^1\text{H}$ 3.85 (s, 6H, 4-OCH₃), 3.91 (s, 12H, 2-OCH₃ and 6-OCH₃), 6.17 (s, 4H, H3 and H5), 7.53 (d, $J = 16.4$, 2H, H8), 8.03 (d, $J = 16.4$, 2H, H7), 8.54 (s, 2H, H10). $\delta^{13}\text{C}$ 55.34 (4-OCH₃), 55.77 (2-OCH₃ and 6-OCH₃), 90.70 (C3 and C5), 107.74 (C1), 124.56 (C8), 125.28 (C7), 142.87 (C10), 150.22 (C9), 160.32 (C4), 161.22 (C2 and C6). Crystals of **6** suitable for a diffraction experiment were obtained from the slow evaporation of a CH_2Cl_2 solution.

2.2. X-ray Crystallography. Data collection for compounds **5** (two polymorphs, **5a** and **5b**) and **6** was performed on an Enraf-Nonius Mach 3 diffractometer using Mo-K α radiation ($\lambda = 0.71073$ Å). The CAD-4 EXPRESS software¹⁷ was used for data collection and cell refinement and XCAD-4 for data reduction.¹⁸ For compound **3** (two polymorphs, **3a** and **3b**), data collection was performed on a Bruker AXS SMART APEX CCD diffractometer using Mo-K α radiation ($\lambda = 0.71073$ Å) by ω scans; the data reduction and multiscan absorption correction was performed with the Apex2 v2008 2.4 software.¹⁹ The structures were solved by direct methods using SHELXS-97²⁰ and refined using SHELXL-97:²⁰ hydrogen atoms were restrained to occupy the calculated positions and defined as riding [$\text{CH} = 0.93$ Å and $U_{\text{iso}}(\text{H}) = 1.2 U_{\text{eq}}(\text{C})$ for aromatic CH]. For the analysis of the supramolecular structures, CH bond lengths were normalized to the value derived from neutron diffraction (1.083 Å). After this normalization procedure, PLATON²¹ was used to calculate all intra- and intermolecular contacts. Figures were prepared using MERCURY (version 2.3).²² MCE 2005²³ was used to visualize the residual electron density between the two ethenyl spacers (Figure 11). The experimental details including the results of the refinements are given in Table 1. The numbering scheme can be found in Figure 1. CCDC-797361 (**3a**), 797362 (**3b**), 797363 (**5a**), 797364 (**5b**), and 797365 (**6**) contain the supplementary crystallographic data for this paper. These data can be obtained free of charge from the Cambridge Crystallographic Data Centre.

3. RESULTS AND DISCUSSION

Attempts were made to grow single crystals suitable for XRD of all oligomers using various crystallization techniques: taking into account the solubilities of the oligomers, these comprise the slow evaporation of CH_2Cl_2 , CHCl_3 , and THF solutions, and vapor diffusion of diethyl ether into saturated CH_2Cl_2 , CHCl_3 , and THF solutions. However, only for compounds **3**, **5**, and **6** crystals of sufficient size and quality were obtained. Details of the data collection and structural refinement of compounds **3** (two polymorphs, **3a** and **3b**), **5** (two polymorphs, **5a** and **5b**), and **6** are collected in Table 1. The necessary data for the structures of compounds **1** and **2** were obtained from the CSD,²⁴ refcodes STPYAZ01 (polymorph **1a**, γ -form),¹⁰ STPYAZ (polymorph **1b**, α -form),¹¹ FUGYAH (polymorph **2a**, γ -form),¹² and FUGYAH01 (polymorph **2b**, α -form).¹² No crystals suitable for a diffraction experiment could be obtained for compound **4**. For all structures, the carbon–hydrogen distances were normalized to 1.083 Å after the refinement, and the resulting geometrical parameters have been used in the following discussion of the different intermolecular short contacts. The details of these contacts have been summarized in Table 2. The numbering scheme of the molecules is given in Figure 1.

All oligomers adopt the anti conformation in which the two ethenyl spacers are oriented in opposite directions with respect to the central pyrazine ring. Also, they adopt the conformation in which the N···N axis in the central ring is aligned with the orientations of the ethenyl links, which was earlier determined to be the more stable.²⁵ Disorder associated with the typical pedal

Table 1. Details of the Data Collection and Structural Refinement of 3a, 3b, 5a, 5b, and 6

	3a	3b	5a	5b	6
A. Crystal Data					
chemical formula	C ₂₄ H ₂₄ N ₂ O ₄	C ₂₄ H ₂₄ N ₂ O ₄	C ₂₆ H ₂₈ N ₂ O ₆	C ₂₆ H ₂₈ N ₂ O ₆	C ₂₆ H ₂₈ N ₂ O ₆
chemical formula weight (g mol ⁻¹)	404.45	404.45	464.50	464.50	464.50
cell setting	monoclinic	monoclinic	monoclinic	monoclinic	monoclinic
space group	<i>P</i> 2 ₁ / <i>c</i>	<i>P</i> 2 ₁ / <i>c</i>	<i>P</i> 2 ₁ / <i>c</i>	<i>P</i> 2 ₁ / <i>c</i>	<i>P</i> 2 ₁ / <i>c</i>
crystal form	plate	prism	needle	block	block
crystal size (mm)	0.05 × 0.38 × 0.55	0.70 × 0.52 × 0.46	0.24 × 0.18 × 0.18	0.34 × 0.32 × 0.32	0.21 × 0.21 × 0.42
crystal color	yellow-green	orange	orange	yellow	orange
no. of reflections for cell param	2867	845	25	25	25
θ -range (°)	2.89–31.08	2.60–22.09	5.20–13.01	5.84–16.52	5.53–11.50
<i>F</i> (0 0 0)	428	428	492	492	492
<i>T</i> (K)	295(2)	295(2)	293(2)	293(2)	293(2)
<i>a</i> (Å)	13.0095(10)	14.118(3)	4.371(2)	8.040(2)	4.389(4)
<i>b</i> (Å)	7.0463(6)	9.424(2)	13.193(4)	10.806(4)	15.4880(10)
<i>c</i> (Å)	12.2219(9)	7.8733(18)	20.695(5)	15.268(5)	17.215(4)
α (°)	90	90	90	90	90
β (°)	115.8140(10)	90.938(5)	98.52(3)	117.533(19)	103.90(3)
γ (°)	90	90	90	90	90
<i>V</i> (Å ³)	1008.57(14)	1047.4(4)	1180.2(7)	1176.2(7)	1136.0(11)
<i>Z</i>	2	2	2	2	2
<i>D</i> _x (Mg m ⁻³)	1.332	1.282	1.307	1.312	1.358
μ (mm ⁻¹)	0.091	0.088	0.093	0.094	0.097
B. Data collection					
diffractometer	Bruker AXS SMART APEX CCD	Bruker AXS SMART APEX CCD	Enraf–Nonius Mach3	Enraf–Nonius Mach3	Enraf–Nonius Mach3
data collection method	ω scans	ω scans	$\omega/2\theta$ scans	$\omega/2\theta$ scans	$\omega/2\theta$ scans
no. of measured reflections	9843	5406	4801	4503	4639
no. of independent reflections	2496	2566	2162	2164	2084
no. of observed reflections	1930	1352	945	776	1330
criterion for observed reflections	<i>I</i> > 2 σ (<i>I</i>)	<i>I</i> > 2 σ (<i>I</i>)	<i>I</i> > 2 σ (<i>I</i>)	<i>I</i> > 2 σ (<i>I</i>)	<i>I</i> > 2 σ (<i>I</i>)
θ_{\max} (°)	28.28	28.28	25.33	25.61	25.34
range of <i>h</i>	−17 ≤ <i>h</i> ≤ 17	−11 ≤ <i>h</i> ≤ 18	−5 ≤ <i>h</i> ≤ 0	0 ≤ <i>h</i> ≤ 9	0 ≤ <i>h</i> ≤ 5
range of <i>k</i>	−9 ≤ <i>k</i> ≤ 9	−12 ≤ <i>k</i> ≤ 12	−15 ≤ <i>k</i> ≤ 15	−13 ≤ <i>k</i> ≤ 13	−18 ≤ <i>k</i> ≤ 18
range of <i>l</i>	−16 ≤ <i>l</i> ≤ 16	−10 ≤ <i>l</i> ≤ 10	−24 ≤ <i>l</i> ≤ 24	−18 ≤ <i>l</i> ≤ 16	−20 ≤ <i>l</i> ≤ 20
no. of standard reflections	0	0	3	3	3
frequency of standard reflections (h)			1	1	1
intensity decay (%)			5	59	1
C. Refinement					
refinement on	<i>F</i> ²	<i>F</i> ²	<i>F</i> ²	<i>F</i> ²	<i>F</i> ²
GOF	1.046	1.047	0.994	0.933	1.019
wR_2	0.1260	0.1740	0.1557	0.2494	0.1008
<i>R</i> ₁	0.0421	0.0612	0.0483	0.0736	0.0343
<i>R</i> _{all}	0.0569	0.1170	0.1571	0.2265	0.0748
no. of reflections used in refinement	2496	2566	2162	2164	2084
no. of parameters used	138	138	157	157	157
weighting scheme	(F _o ²) + (AP) ² + BP] where P = (F _o ² + 2F _c ²)/3				
<i>A</i>	0.0625	0.0660	0.0594	0.1245	0.0424
<i>B</i>	0.1472	0.0637	0.1671	0.00	0.1907
(Δ / σ) _{max}	0.00	0.00	0.00	0.00	0.00
$\Delta\rho_{\max}$	0.252	0.186	0.161	0.477	0.132
$\Delta\rho_{\min}$	−0.180	−0.163	−0.205	−0.235	−0.124

Table 2. Details (distances d in Å, angles θ in degrees and symmetry codes) of the Short Intermolecular Contacts D–H...A Given in the Text^a

	D	H	A	$d_{H...A}$	$d_{D...A}$	θ	symmetry code
1a	C10	H10	N1D	2.57	3.452	139	$x, y, -1 + z$
	C10D	H10D	N1	2.55	3.460	140	$x, y, 1 + z$
	C6D	H6D	Cg(Ar)	2.80	3.536	125	$-x, -y, -z$
	C5D	H5D	N1D	2.70	3.682	150	$1/2 - x, 1/2 + y, -z$
1b	C6	H6	N1	2.66	3.719	167	$-x, 1/2 + y, -1/2 - z$
	C4	H4	Cg(Ar)	2.85	3.876	159	$1/2 - x, -y, -1/2 + z$
2a	C10	H10	N1	2.50	3.366(2)	136	$x, 1 + y, z$
	C41	H41b	O4	2.49	3.429(1)	145	$1/2 - x, 1/2 - y, 1 - z$
	C41	H41a	Cg(Ar)	2.47	3.484(2)	155	$x, -y, -1/2 + z$
2b	C6	H6	N1	2.58	3.633(2)	163	$1/2 - x, y, -1/2 + z$
	C41	H41b	O4	2.64	3.725(2)	179	$x, 3/2 - y, -1/2 + z$
	C10	H10	C7=C8	2.70	3.653(2)	147	$-1/2 - x, y, 1/2 + z$
	C41	H41c	C7=C8	2.76	3.809(2)	165	$x, y, -1 + z$
3a	C41	H41b	O3	2.48	3.475(2)	152	$1 - x, 1 - y, 1 - z$
	C6	H6	Cg(Ar _N)	2.68	3.433(2)	126	$x, 1/2 - y, -1/2 + z$
	C10	H10	Cg(Ar)	2.75	3.518(2)	128	$-x, -1/2 + y, 3/2 - z$
3b	C41	H41b	O3	2.58	3.614(3)	158	$2 - x, 2 - y, -z$
	C31	H31b	O4	2.57	3.585(5)	155	$2 - x, -1/2 + y, 1/2 - z$
	C31	H31c	O4	2.46	3.316(5)	135	$x, 3/2 - y, 1/2 + z$
	C6	H6	N1	2.55	3.553(3)	154	$x, 5/2 - y, -1/2 + z$
	C41	H41c	Cg(Ar)	2.85	3.742(3)	139	$x, 5/2 - y, -1/2 + z$
5a	C41	H41a	O4	2.37	3.230(5)	136	$-1 + x, y, z$
	C41	H41c	O3	2.62	3.346(5)	123	$-1 + x, y, z$
	C2	H2	O4	2.70	3.774(4)	172	$-x, 1/2 + y, 1/2 - z$
	C31	H31a	O4	2.67	3.292(4)	116	$-x, 1/2 + y, 1/2 - z$
	C10	H10	O3	2.53	3.389(4)	135	$x, 1/2 - y, 1/2 + z$
	C41	H41b	C7=C8	2.75	3.540(6)	130	$-1 - x, -1/2 + y, 1/2 - z$
5b	C2	H2	O5	2.68	3.688(8)	155	$x, 1/2 - y, -1/2 + z$
	C8	H8	O5	2.45	3.460(7)	154	$x, 1/2 - y, -1/2 + z$
	C6	H6	O4	2.58	3.478(7)	140	$-x, 1/2 + y, 1/2 - z$
	C7	H7	O4	2.61	3.503(8)	139	$-x, 1/2 + y, 1/2 - z$
6	C7	H7	O6	2.28	2.700(2)	100.9	intramolecular
	C8	H8	O2	2.12	2.805(2)	118.5	intramolecular
	C41	H41b	O6	2.70	3.684(3)	151	$-1 + x, -1/2 - y, -1/2 + z$
	C41	H41c	N1	2.52	3.479(3)	147	$-1 + x, -1/2 - y, -1/2 + z$
	C21	H21a	O4	2.52	3.482(3)	147	$1 - x, -y, -z$
	C21	H21c	Cg(Ar)	2.96	3.873(4)	142	$-1 + x, y, z$
	C61	H61c	Cg(Ar)	2.99	3.860(4)	137	$1 + x, y, z$

^a The lack of an esd on a number of the parameters is due to the normalization of the CH distances and/or the absence of esds in the CIFs of **1a** and **1b**.

motion of the ethenyl spacers²⁶ could not be identified in any of the five new solid-state structures. In the following, the crystal structures of **1** and **2** will be reviewed and compared in detail, after which the structures of the new compounds (**3–6**) will be analyzed.

3.1. *E,E*-2,5-Bis(2-phenylethenyl)pyrazine (1). Molecules in the γ -form (**1a**) of **1** are noncentrosymmetric and twisted along the molecular axis (Figure 3). This can be seen most clearly from the different dihedral angles between the least-squares planes through the rings. The angle between the plane through peripheral ring A and the plane through the central ring is about 27°, while the angle between the plane through the central ring and the plane through peripheral ring B is about 25°. In contrast, molecules in the α -form (**1b**) of **1** are

virtually planar and centrosymmetric: the central pyrazine ring is twisted out of the plane of the peripheral benzene ring by about 12°.

In the γ -form (**1a**) typical pyrazine chains based on the synthon in Figure 2b are formed in the [0 0 1] direction, and the peripheral rings are twisted out of the plane of the pyrazine ring to accommodate the C10–H10...N1D and C10D–H10D...N1 hydrogen bonds (Figure 3). These chains are then held together two by two by a CH... π interaction [C6D–H6D...Cg(Ar)] and form stacks perpendicular to the chains. Finally, these stacks of coupled chains are linked by weak hydrogen bonds [C5D–H5D...N1D] (not given in Figure 3).

In the α -form (**1b**) the molecules organize themselves into sawtooth ribbons in the [0 1 0] direction through weak CH...N

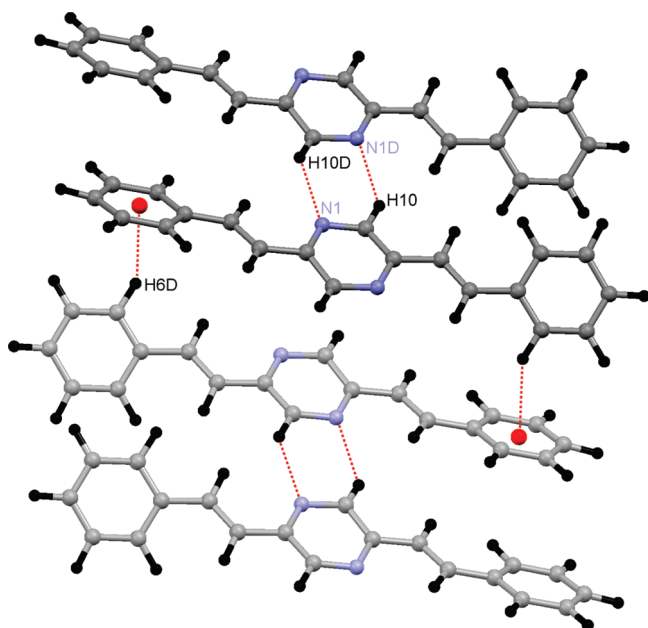


Figure 3. The typical pyrazine chain in the $[0\ 0\ 1]$ direction and the $\text{CH}\cdots\pi$ interaction between the layers in the γ -form of **1** (polymorph **1a**).

hydrogen bonds also involving the nitrogen atoms of the pyrazine rings $[\text{C6}-\text{H6}\cdots\text{N1}]$, but these are different from the typical synthons given in Figure 2b (Figure 4a). Perpendicular to these ribbons the $\pi\cdots\pi$ stacks based on the synthon in Figure 2a are formed which are responsible for the photoactivity of the structure: the $\text{Cg}(\text{Ar}_\text{N})\cdots\text{Cg}(\text{Ar})$ distance is 3.940 Å (Figure 4b,c). Finally, these stacks assemble in a herringbone pattern held together by a weak hydrogen bond in which H4 contacts the centroid of a phenyl ring $[\text{C4}-\text{H4}\cdots\text{Cg}(\text{Ar})]$ (Figure 4a,c).

3.2. *E,E*-2,5-Bis[2-(4-methoxyphenyl)ethenyl]pyrazine (2**).** Molecules in both the γ - (**2a**) α -forms (**2b**) of **2** are relatively planar: the least-squares plane through the central pyrazine ring makes an angle of about 30° with the plane through the peripheral benzene ring in **2a**, while this angle is limited to about 15° in **2b**.

In the γ -form (**2a**), typical pyrazine chains based on the synthon in Figure 2b are formed in the $[0\ 1\ 0]$ direction and the peripheral rings are twisted out of the plane of the pyrazine ring to accommodate the $\text{C10}-\text{H10}\cdots\text{N1}$ hydrogen bonds (Figure 5a). These chains are then interconnected through methoxy \cdots methoxy dimer formation $[\text{C41}-\text{H41b}\cdots\text{O4}]$ in the direction perpendicular to the chains, constructing sheets of molecules. Finally, these sheets are organized into shifted stacks through $-\text{OCH}_3\cdots\pi$ interactions $[\text{C41}-\text{H41a}\cdots\text{Cg}(\text{Ar})]$ (Figure 5b).

In the α -form (**2b**) the molecules organize themselves into sawtooth ribbons through weak hydrogen bonds also involving the nitrogen atoms of the pyrazine ring $[\text{C6}-\text{H6}\cdots\text{N1}]$, but these are different from the typical synthons given in Figure 2b (Figure 6a). Perpendicular to these ribbons the $\pi\cdots\pi$ stacks based on the corresponding synthon (Figure 2a) are formed which are responsible for the photoactivity of the structure: the $\text{Cg}(\text{Ar}_\text{N})\cdots\text{Cg}(\text{Ar})$ distance is 3.988 Å (Figure 6b,c). Finally, these stacks assemble in a herringbone pattern held together by weak $\text{CH}\cdots\text{O}$ hydrogen bonds between the methoxy groups $[\text{C41}-\text{H41b}\cdots\text{O4}]$ (Figure 6a,c). As a consequence of this three-dimensional organization, two additional but very weak interactions can be identified: H41b and H10 contact the π -system of one of the vinyl spacers (Figure 6a).

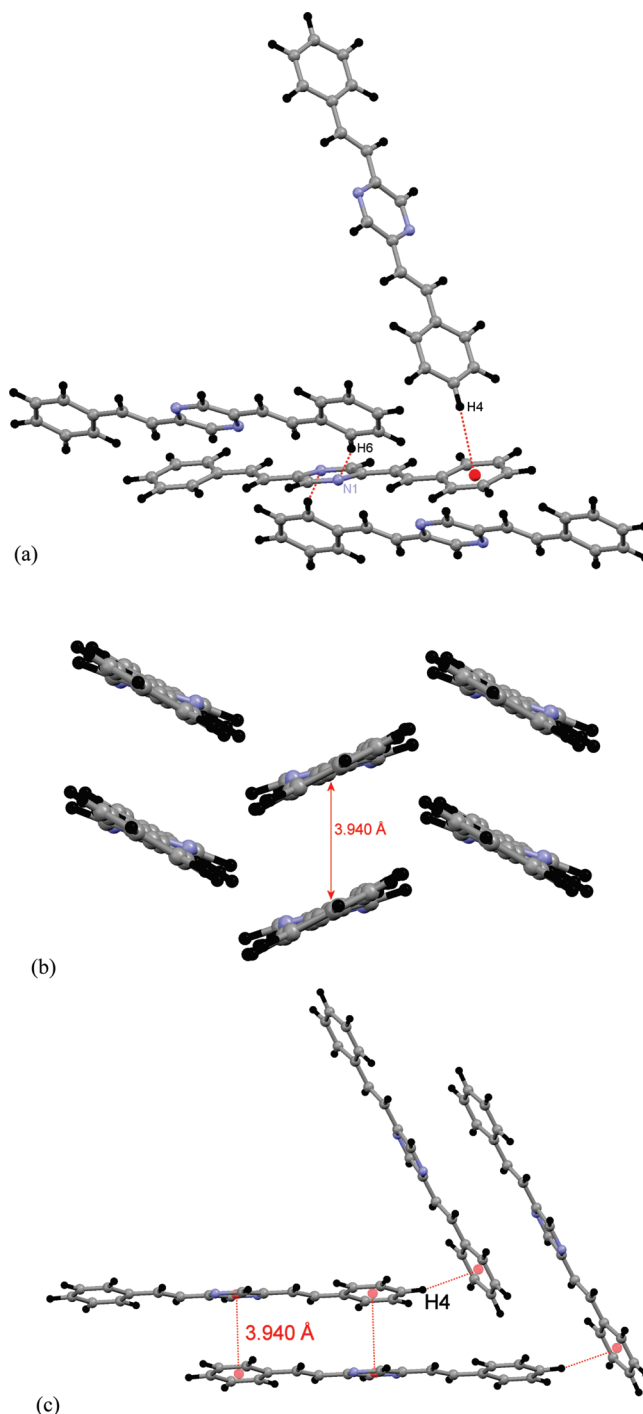


Figure 4. (a) Sawtooth organization of the molecules, (b) weak interactions between the molecules, and (c) $\pi_{\text{pyrazine}}\cdots\pi_{\text{phenyl}}$ stacking in the α -form of **1** (polymorph **1b**).

3.3. The Analogy between the Packings of **1 and **2**.** The 2,5-distyrylpyrazine unit has two particular properties which determine its supramolecular behavior. First, there is the C–H bond on the central ring which is activated by the presence of the electron-withdrawing nitrogen atom. This directly leads to the possibility of generating relatively strong reciprocal $\text{CH}\cdots\text{N}$ hydrogen bonds between two molecules in the synthon depicted in Figure 2b. Second, it consists of an electron-poor central pyrazine ring (at least with respect to the peripheral benzene

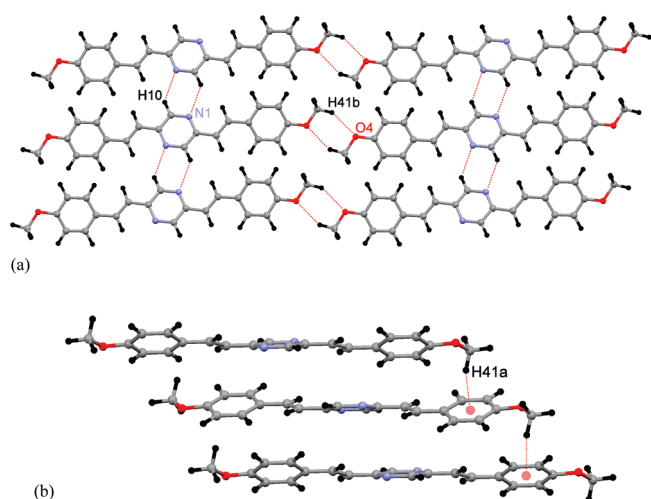


Figure 5. (a) The combination of the hydrogen-bonded synthon with the methoxy...methoxy interactions leading to sheets, and (b) the CH... π interactions stacking these sheets in the γ -form of **2** (polymorph **2a**).

rings) and two electron-rich peripheral benzene rings (at least with respect to the central pyrazine ring). This directly leads to the possibility of generating favorable π ... π interactions in the synthon depicted in Figure 2a, by stacking the molecules perpendicularly and shifting them the length of a styryl fragment. Clearly, each of these two properties lies at the basis of one of the three-dimensional structures observed in the two polymorphs, in this case **1a** and **1b**, respectively. The introduction of methoxy groups in both 4-positions of the benzene rings will increase the polarization of the molecules, as they enhance the electron-richness of the peripheral rings. How they influence the expression of the two properties mentioned above can be seen from the comparison of the supramolecular structures of **1** and **2**.

In **1a** and **2a** the pyrazine hydrogen-bonded synthon (Figure 2b) generates the main building blocks of the crystal in the form of the chains (Figures 3 and 5a). Then, the CH... π interactions holding these chains together in **1a** are replaced by -OCH₃... π interactions in **2a** (Figures 3 and 5b). Finally, the CH...N interactions interconnecting the stacks in **1a** are replaced by methoxy...methoxy contacts (Figure 5a) in **2a**; this tendency of methoxy groups to favor reciprocal contacts is known, as it has been identified in the crystal structures of methoxy-substituted distyrylbenzenes.^{15,16} As such, the methoxy groups in **2a** take over the role of a number of hydrogen atoms in **1a**, but do not fundamentally change the supramolecular organization.

Similarly, from a juxtaposition of Figures 4 and 6 the resemblance of the packing motifs of **1b** and **2b** becomes clear. In these polymorphs the $\pi_{\text{pyrazine}} \cdots \pi_{\text{phenyl}}$ synthon (Figure 2a) generates the main building blocks of the crystal in the form of the stacks (Figures 4b and 6b). Then, in both **1b** and **2b**, these stacks are interconnected into stacked ribbons via CH...N contacts, which are, as mentioned earlier, different from the synthons given in Figure 2b (Figures 4a and 6a). Finally, the stacked ribbons are organized into a herringbone pattern based on different T-shaped interactions. These are the CH... π interactions in **1b** involving the *para*-CH moiety from the peripheral benzene rings (Figure 4a,c), which are replaced by methoxy...methoxy contacts involving the *para*-methoxy groups (Figure 6a,c) in **2b**; again, the methoxy groups favor the formation of reciprocal contacts.^{15,16} The similarities between the crystal packings of **1b**

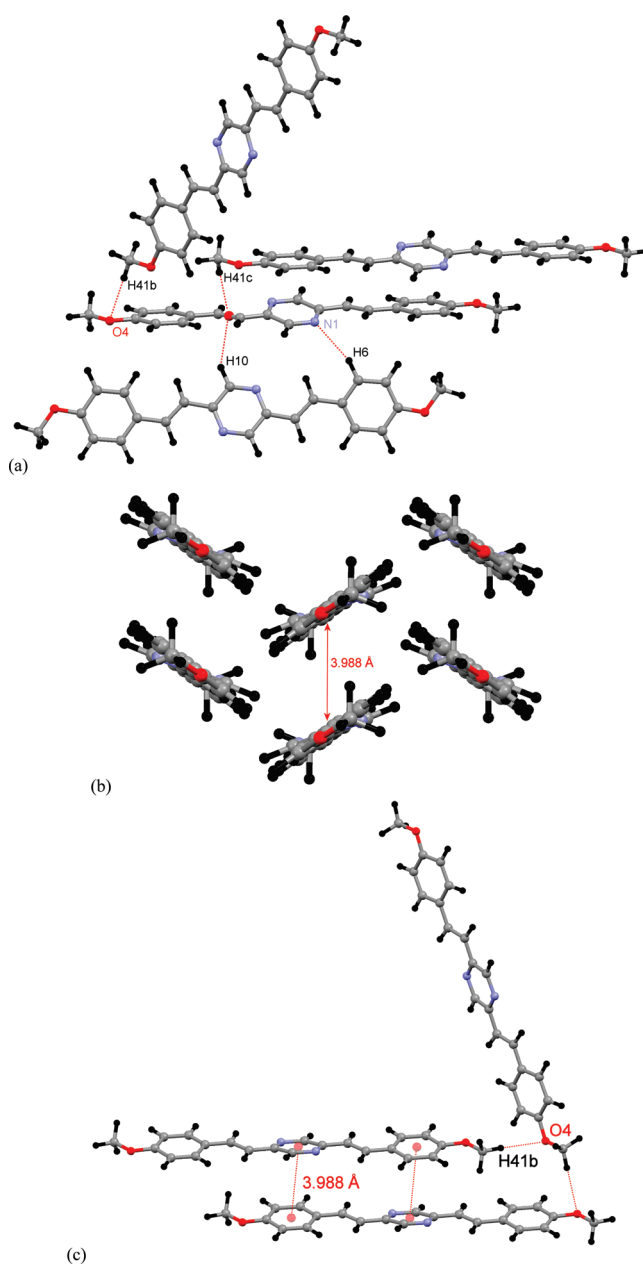


Figure 6. (a) Sawtooth organization of the molecules, (b) weak interactions between the molecules, and (c) $\pi_{\text{pyrazine}} \cdots \pi_{\text{phenyl}}$ stacking in the α -form of **2** (polymorph **2b**).

and **2b**, despite the difference in length of the molecules, can also be recognized in the similarity of the unit cell parameters, since the main sawtooth motif runs along the longest cell axis: 20.638(7) vs 26.061(3) Å, 7.655(6) vs 7.3280(10) Å, and 9.599(6) vs 9.1240(10) Å for **1b** and **2b**, respectively, keeping in mind that the former was studied at room temperature and the latter at 150 K. As in **2a**, the methoxy groups in **2b** take over the role of a number of hydrogen atoms in **1b**, but do not fundamentally change the supramolecular organization. In the following the supramolecular structures of the new compounds containing more than one methoxy groups per peripheral ring will be discussed.

3.4. *E,E*-2,5-Bis[2-(3,4-dimethoxyphenyl)ethenyl]pyrazine (3). Compound **3** crystallized as a mixture of two polymorphs (**3a** and **3b**). In **3a** the angle between the pyrazine and benzene

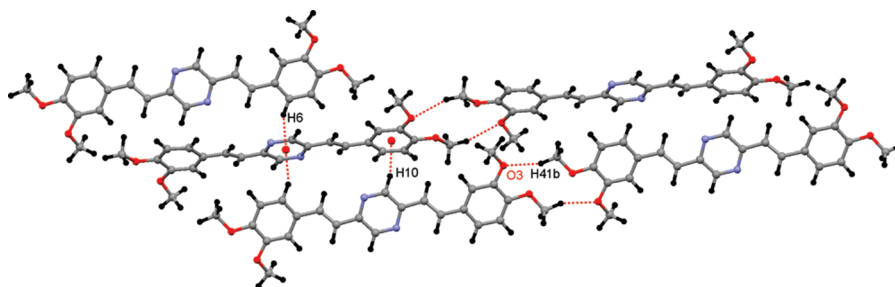


Figure 7. The infinite chains held together by two $\text{CH}\cdots\pi$ contacts in **3a**.

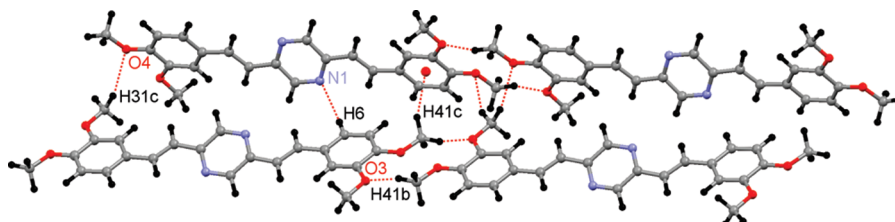


Figure 8. The infinite chains held together by $\text{CH}\cdots\pi$, $\text{CH}\cdots\text{O}$, and $\text{CH}\cdots\text{N}$ contacts in **3b**.

planes is about 6° . The methoxy group in the 3-position is twisted out of the plane of the benzene ring (about 19°) to a greater extent than the one in the 4-position (about 8°); this may be linked to the former's involvement as hydrogen bond acceptor (see below). In **3b** the pyrazine ring is twisted about 23° out of the plane of the benzene ring. The methoxy groups are quasi coplanar with the benzene ring, as torsion angles of about 1° and about 5° are measured for the groups in the 3- and 4-positions, respectively.

In the structure of **3a** (Figure 7), chains of molecules are formed in the $[1\ 0\ \bar{1}]$ direction through two mutual methoxy \cdots methoxy contacts with the methoxy group in the 4-position as hydrogen bond donor and the one in the 3-position as acceptor: H41b contacts the oxygen atom of the methoxy group in the 3-position [C41–H41b \cdots O3]. These chains are then organized into the three-dimensional structure via two different $\text{CH}\cdots\pi$ interactions: H6 contacts the pyrazine ring [C6–H6 \cdots Cg(Ar_N)], whereas H10 contacts the methoxy-substituted ring [C10–H10 \cdots Cg(Ar)].

A similar situation is found in the second polymorph **3b** (Figure 8). Again, chains of molecules are formed through involvement of the methoxy groups in the 3- and 4-positions as acceptors and donors, respectively [C41–H41b \cdots O3]. These chains are now organized into the three-dimensional structure through additional methoxy \cdots methoxy contacts with the methoxy group in the 3-position acting as donor: H31b and H31c contact the oxygen atoms of two 4-methoxy groups from two different molecules (Table 2). In addition to these, further lateral $\text{CH}\cdots\text{N}$ and $\text{CH}\cdots\pi$ contacts can be seen between H6 and the nitrogen atom of the pyrazine ring [C6–H6 \cdots N1] and between H41c and the π -system of the methoxy-substituted ring [C41–H41c \cdots Cg(Ar)], respectively. Note that the relatively acidic H10 does not participate in this packing, while it did in **3a**.

3.5. *E,E*-2,5-Bis[2-(3,4,5-trimethoxyphenyl)ethenyl]pyrazine (5**).** Compound **5** crystallized as a mixture of two polymorphs (**5a** and **5b**). In **5a** the plane of the pyrazine ring makes an angle of about 10° with the plane of the benzene ring; in **5b** this angle is about 15° . Neither angle is actually due to a twist of

the molecules along the molecular axis, as in the previously discussed compounds and polymorphs, but rather a consequence of the peculiar *Z* shape of the molecules which was also seen in both *E,E*-1,4-bis[2-(3,4,5-trimethoxyphenyl)ethenyl]benzene (CSD refcode JACBIY²⁷) and *E,E*-2,5-dimethoxy-1,4-bis-[2-(3,4,5-trimethoxyphenyl)ethenyl]benzene (CSD refcode GAKZAU¹⁵); these two compounds can be considered the DSB analogues of **5**. Because of the 3,4,5-trisubstitution on the peripheral rings, the methoxy groups in the 4-position are almost perpendicular (about 85°) to the benzene ring, while those in the 3- and 5-positions remain in the plane, making angles of about 5° and 6° , in **5a**; in **5b** these values are about 86° , 3° , and 4° , respectively.

In the structure of **5a** (Figure 9) shifted stacks of molecules are generated through two methoxy \cdots methoxy weak hydrogen bonds [C41–H41a \cdots O4 and C41–H41c \cdots O3] (Figure 9a). These stacks are then connected to each other by three weak hydrogen bonds [C2–H2 \cdots O4, C31–H31a \cdots O4, and C10–H10 \cdots O3] (Figure 9b). In addition, H41b of the methoxy group in the 4-position contacts the π -system of the ethenyl spacer of a molecule above (not given in Figure 9). All three hydrogen atoms of this *para*-methoxy group are used in developing the crystal structure, while the methoxy group in the 5-position remains unused.

In **5b**, however, no methoxy \cdots methoxy contacts are present (Figure 10). Aromatic and ethenyl hydrogen atoms H2 and H8 contact O5, while on the other side of the molecule H6 and H7 contact O4 (Table 2). Because of the presence of the face-to-face synthon (Figure 2a), the relatively acidic H10 does not take part in the intermolecular network. The pronounced $\pi_{\text{pyrazine}} \cdots \pi_{\text{phenyl}}$ interactions with a Cg(Ar_N) \cdots Cg(Ar) distance of 3.859 Å are easily recognized and are the reason for this structure to meet the criteria for a solid-state polymerization: the ethenyl spacers are only 3.367 Å apart which is well below the 4.2 Å criterion. Indeed, during the measurement a large intensity decay of the control reflections could be observed (Table 1). During the refinement residual electron density could be located in the neighborhood of the ethenyl spacers and this is graphically represented in Figure 11. Furthermore, upon inspection of the crystal after the measurement it was found to have changed from a yellow block to a white mass.

All these observations clearly indicate this polymorph's photosensitivity. There was not enough material for any kind of further analysis of the photoproduct.

3.6. *E,E*-2,5-Bis[2-(2,4,6-trimethoxyphenyl)ethenyl]pyrazine (6). In **6** the plane of the pyrazine ring and the plane of the benzene ring make an angle of about 9° , and this seems to be the result of the combination of a twist along the molecular axis, as in **1**, **2**, and **3**, and a slight Z shape, as in **5**. The three methoxy groups deviate by no more than about 5° from the plane of the

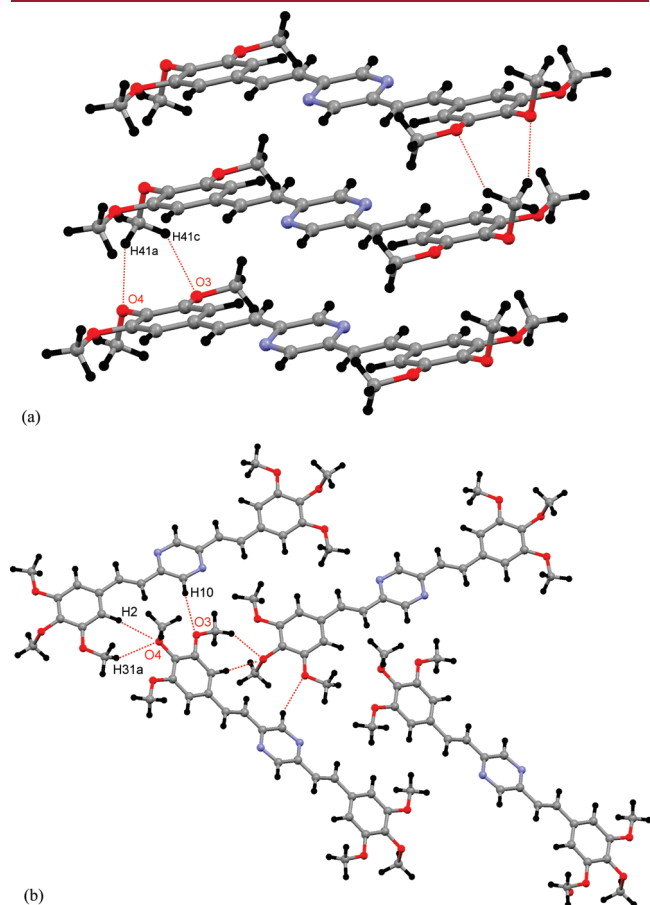


Figure 9. (a) The shifted stacks based on methoxy \cdots methoxy interactions and (b) the herringbone pattern generated by CH \cdots O contacts in **5a**.

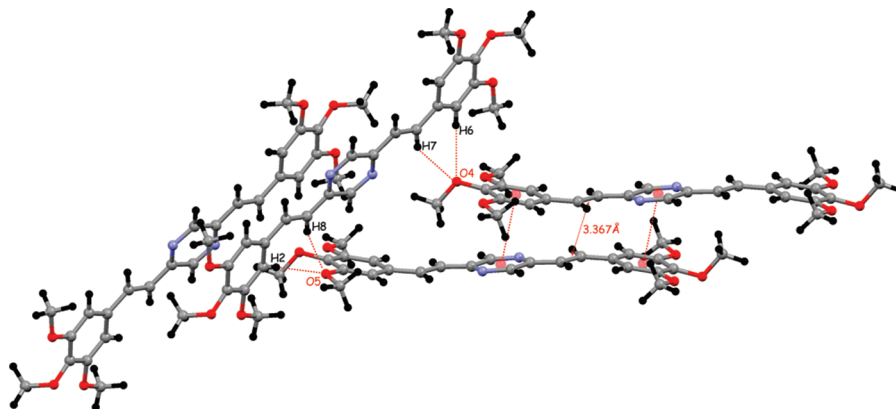


Figure 10. The polymerizable chains based on the $\pi_{\text{pyrazine}} \cdots \pi_{\text{phenyl}}$ synthon, and the CH \cdots O contacts which connect the chains in **5b**.

benzene ring, and for those in the 2- and 6-positions this may be linked to their involvement in intramolecular CH \cdots O interactions (Table 2).²⁸

The molecules in **6** are interconnected by the methoxy group in the 4-position which simultaneously contacts N1 and O6 (Figure 12a). The methoxy group in the 2-position forms a typical methoxy \cdots methoxy interaction with the oxygen atom of the methoxy group in the 4-position [C21–H21a \cdots O4] (Figure 12b). Stairlike stacks are then formed by CH \cdots π contacts involving the methoxy groups in the 2- and 6-positions and the C21–H21a \cdots O4 contact mentioned above (Figure 12b). Again, H10 is not used.

3.7. The Supramolecular Structures of Methoxy-Substituted Distyrylpyrazines. The first expected effect of the introduction of more than one methoxy group on each of the two peripheral rings, that is, the switching off of the typical pyrazine hydrogen-bonded synthon (Figure 2b) seen in **1a** and **2a**, has clearly been achieved: in none of the five structures of compounds **3**, **5**, and **6** this synthon can be observed. In fact, the nitrogen atom has been relegated to a very subordinate role. Only in **3b** and **6** is it involved as acceptor in CH \cdots N contacts: in the former the donor is the same methine group of one of the peripheral benzene rings as in **1b** and **2b**, and in the latter the donor is a methoxy group. Note that to form the CH \cdots N hydrogen bonds of the pyrazine chain (Figure 2b), **1**, **2** and *E,E*-2,5-bis[2-(2,3,4,5,6-pentafluorophenyl)ethenyl]pyrazine²⁵ (the decafluoro derivative of **1**) twist their peripheral rings out of the plane of the pyrazine ring to reduce the intermolecular

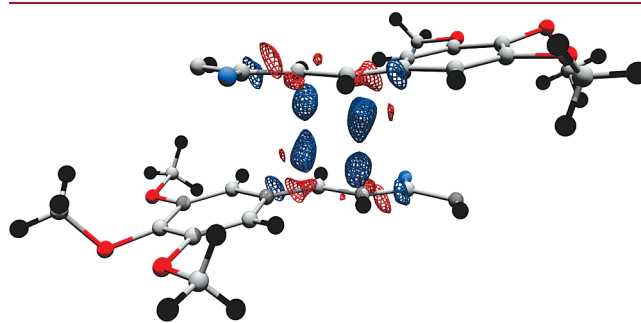


Figure 11. Residual electron density appearing between the ethenyl spacers of two neighboring molecules in polymorph **5b**; contour surfaces are plotted at $0.8 \text{ e } \text{Å}^{-3}$ (blue) and $-0.8 \text{ e } \text{Å}^{-3}$ (red). Note that only one-half of each of the molecules is represented.

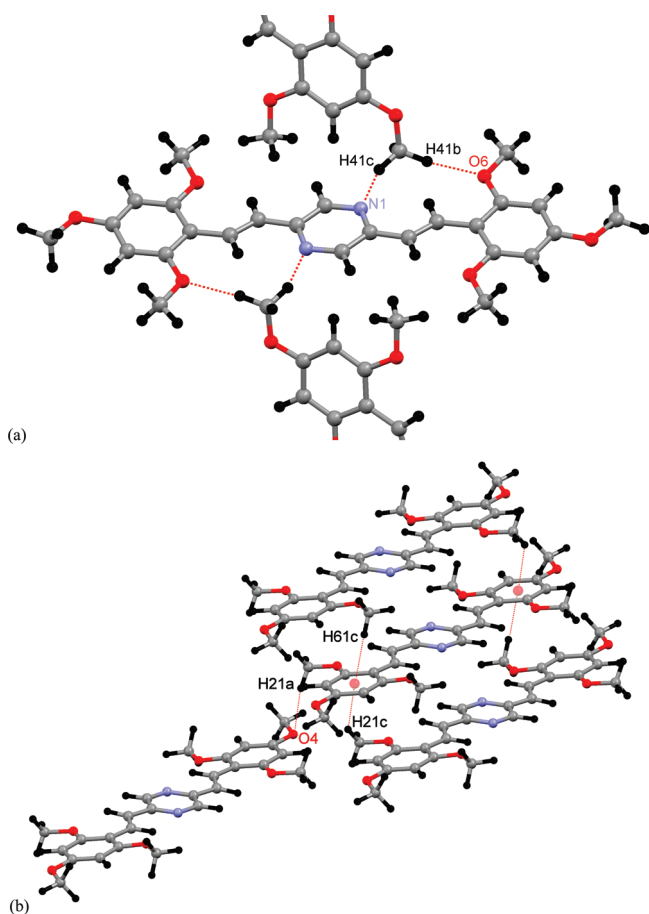


Figure 12. (a) The intermolecular contacts between the methoxy group in the 4-position and N1 and O6 (the top and bottom molecules have been only partially represented), and (b) the stairlike stacks formed by $\text{CH}\cdots\pi$ contacts in **6**.

distance; this option is not used by any of the other DSPs under investigation.

The second expected effect, the switching off of the $\pi_{\text{pyrazine}}\cdots\pi_{\text{phenyl}}$ synthon (Figure 2a) seen in **1b** and **2b**, as a result of the increased number of favored reciprocal methoxy \cdots methoxy contacts, has also been achieved, at least in part: in just one (**5b**) of the five structures of compounds **3**, **5**, and **6** this synthon can be observed. Indeed, our earlier suggestion^{15,16} that methoxy groups tend to favor contacts among each other in methoxy-substituted DSPs can now be extended to include three DSPs (besides **2**), as the supramolecular structures of **3a**, **3b**, **5a**, and **6** all depend heavily on intermolecular $\text{CH}\cdots\text{O}$ contacts between methoxy groups. In **3a** and **3b** these interactions lead to the formation of the chains of molecules (Figures 7 and 8), and in **3b** two extra methoxy \cdots methoxy contacts assist in the organization of these chains into the observed three-dimensional structure (Figure 8). In **5a** one such contact assists in generating the herringbone pattern which interlinks the shifted stacks of molecules (Figure 9b), while these stacks themselves are based on two methoxy \cdots methoxy contacts (Figure 9a). In **6** one such interaction cooperates with the $\text{CH}\cdots\text{N}$ contact mentioned above (Figure 12a), and a second is involved in the formation of the stairlike stacks (Figure 12b).

Besides these methoxy \cdots methoxy contacts these substituents are involved in a second synthon also seen in methoxy-substituted DSPs, that is, $-\text{OCH}_3\cdots\pi$ interactions.^{15,16,28,29}

One such interaction is present in **2a**, in **3b** one works together with the $\text{CH}\cdots\text{N}$ and the two methoxy \cdots methoxy interactions mentioned above, and in **6** two of them join the methoxy \cdots methoxy contact in forming the stairlike stacks. These $-\text{OCH}_3\cdots\pi$ interactions clearly also play a part in preventing the formation of the $\pi_{\text{pyrazine}}\cdots\pi_{\text{phenyl}}$ synthon, thereby assisting the methoxy \cdots methoxy interactions.

Polymorph **5b** clearly sets itself apart from the other four. There are neither methoxy \cdots methoxy nor $-\text{OCH}_3\cdots\pi$ contacts, despite the large number of such groups; two of the methoxy groups are involved as acceptor in four $\text{CH}\cdots\text{O}$ interactions with C–H bonds of the peripheral rings and the ethenyl spacers. The absence of methoxy \cdots methoxy or $-\text{OCH}_3\cdots\pi$ contacts allows the structure to switch on the $\pi_{\text{pyrazine}}\cdots\pi_{\text{phenyl}}$ synthons, leading to its observed photoinstability. As **5** and **6** contain the same number of methoxy groups, their relative positions must be the reason for their different behavior. Indeed, both **5** and **6** enjoy the enhanced polarization of the DSP backbone due to the increased number of electron-donating groups, favoring the $\pi\cdots\pi$ synthon, but in **6** the methoxy group in the 6-position collaborates with the nitrogen atom of the pyrazine ring to create a “pocket” of increased electron density in which the 4-methoxy group gladly positions itself, thereby efficiently eliminating the possibilities for $\pi\cdots\pi$ stacking. The structure then reverts to using $-\text{OCH}_3\cdots\pi$ contacts as the main organizational tool, just like *E,E*-2,5-dimethoxy-1,4-bis[2-(2,4,6-trimethoxyphenyl)ethenyl]benzene (CSD refcode BEZYAH²⁸), its most closely related DSP analogue. The absence of methoxy groups in the 2- and 6-positions and the rather awkward orientation of the methoxy group in the 4-position prevent **5** from adopting a similar structure, which leaves the door wide open for $\pi\cdots\pi$ stacking in **5b**.

Finally, even though our crystal engineering approach succeeded in dispensing with the polymorphs based on the typical pyrazine hydrogen-bonded synthon and the $\pi_{\text{pyrazine}}\cdots\pi_{\text{phenyl}}$ synthon (at least for two of the three compounds), the introduction of more methoxy substituents did not lead to the exclusion of polymorphism, that is, a situation in which one polymorph is considerably more energetically favorable than any other. The two polymorphic modifications of **3** are remarkably similar: in both structures infinite chains are formed via the methoxy groups in the 4-positions contacting the methoxy groups in the 3-positions. Then, the main difference between **3a** and **3b** is the manner in which these chains are held together: in **3a** this is achieved by two $\text{CH}\cdots\pi$ contacts, while in **3b** only one $\text{CH}\cdots\pi$ contact exists next to two $\text{CH}\cdots\text{O}$ and one $\text{CH}\cdots\text{N}$ weak hydrogen bonds. On the other hand, the two polymorphic modifications of **5** are considerably more different. While the structure of **5a** is mainly dictated by weak hydrogen bonds involving the methoxy groups, in **5b** the $\pi_{\text{pyrazine}}\cdots\pi_{\text{phenyl}}$ synthon is favored over methoxy \cdots methoxy interactions.

4. CONCLUSIONS

A clear analogy between the structures and polymorphs of *E,E*-2,5-bis(2-phenylethenyl)pyrazine (**1**) and *E,E*-2,5-bis[2-(4-methoxyphenyl)ethenyl]pyrazine (**2**) has emerged from a detailed comparison of their supramolecular structures. The addition of one methoxy group to each of the benzene rings upon going from **1** to **2** proved to be a small enough change for **2** to assimilate both possible crystal packings of **1**, based on the pyrazine chain and $\pi_{\text{pyrazine}}\cdots\pi_{\text{phenyl}}$ synthons. The pyrazine

hydrogen-bonded synthon is easily deactivated by the further addition of one or two methoxy group(s) to each of the peripheral rings in a position other than the para position. However, the $\pi \cdots \pi$ synthon, which brings about a photosensitive structure, can only be switched off if the methoxy groups can dominate the supramolecular structure through reciprocal interactions, as in **3a**, **3b** and **5a**, or via favorable interactions with the nitrogen atom, as in the “pocket” of increased electron density in the structure of **6**. In general, though, the role of the nitrogen atom has become subordinate, and it is no longer the driving force behind the observed three-dimensional organization, which it is in **1** and **2**. Thus, the crystal engineering strategy in which methoxy groups are used to generate intermolecular $\text{CH} \cdots \text{O}$ and $-\text{OCH}_3 \cdots \pi$ contacts and switch off others has been successful. On the other hand, polymorphism remains: based on the fact that four sets of polymorphs were observed for five compounds, it is clear that polymorphism and distyrylpyrazines are closely associated.

■ ASSOCIATED CONTENT

S **Supporting Information.** Synthesis details for **2** and **4**; crystallographic information file. This material is available free of charge via the Internet at <http://pubs.acs.org>.

■ AUTHOR INFORMATION

Corresponding Author

*Fax +32.3.265.23.10, e-mail frank.blockhuys@ua.ac.be.

■ ACKNOWLEDGMENT

A.C. wishes to thank the Institute for the Promotion of Innovation by Science and Technology in Flanders (IWT) for his predoctoral grants. Financial support by FWO-Vlaanderen under Grant G.0129.05 and by the University of Antwerp under Grant GOA-2404 is gratefully acknowledged.

■ REFERENCES

- (1) Tachelet, W.; Jacobs, S.; Ndayikengurukiye, H.; Geise, H. J.; Gruner, J. *App. Phys. Lett.* **1994**, *64*, 2364–2366.
- (2) Jin, Y. D.; Yang, J. P.; Heremans, P. L.; Van der Auweraer, M.; Rousseau, E.; Geise, H. J.; Borghs, G. *Chem. Phys. Lett.* **2000**, *320*, 387–392.
- (3) Yang, J. P.; Heremans, P. L.; Hoefnagels, R.; Tachelet, W.; Dieltiens, P.; Blockhuys, F.; Geise, H. J.; Borghs, G. *Synth. Met.* **2000**, *108*, 95–100.
- (4) Yang, J. P.; Jin, Y. D.; Heremans, P. L.; Hoefnagels, R.; Dieltiens, P.; Blockhuys, F.; Geise, H. J.; Van der Auweraer, M.; Borghs, G. *Chem. Phys. Lett.* **2000**, *325*, 251–256.
- (5) Jin, Y. D.; Chen, H. Z.; Heremans, P. L.; Aleksandrak, K.; Geise, H. J.; Borghs, G.; Van der Auweraer, M. *Synth. Met.* **2002**, *127*, 155–158.
- (6) Chemla, D. S. *Nonlinear Optical Properties of Organic Molecules and Crystals*; Academic Press: Boston, 1987.
- (7) Metzger, R. M.; Chen, B.; Hopfner, U.; Lakshminantham, M. V.; Vuillaume, D.; Kawai, T.; Wu, X. L.; Tachibana, H.; Hughes, T. V.; Sakurai, H.; Baldwin, J. W.; Hosch, C.; Cava, M. P.; Brehmer, L.; Ashwell, G. J. *J. Am. Chem. Soc.* **1997**, *119*, 10455–10466.
- (8) Nohara, M.; Hasegawa, M.; Hosokawa, C.; Tokailin, H.; Kusumoto, T. *Chem. Lett.* **1990**, 189–190.
- (9) Grimdale, A. C.; Cervini, R.; Friend, R. H.; Holmes, A. B.; Kim, S. T.; Moratti, S. C. *Synth. Met.* **1997**, *85*, 1257–1258.
- (10) Nakanishi, H.; Ueno, K.; Sasada, Y. *Acta Crystallogr. B* **1976**, *32*, 3352–3354.

- (11) Sasada, Y.; Shimanou, H.; Nakanishi, H.; Hasegawa, M. *Bull. Chem. Soc. Jpn.* **1971**, *44*, 1262–1270.
- (12) Scaccianoce, L.; Feeder, N.; Teat, S. J.; Marseglia, E. A.; Grimdale, A. C.; Holmes, A. B. *Acta Crystallogr. C* **2000**, *56*, 1277–1279.
- (13) Schmidt, G. M. J.; Penzien, K. *Angew. Chem., Int. Ed.* **1969**, *8*, 608.
- (14) Stezowski, J. J.; Peachey, N. M.; Goebel, P.; Eckhardt, C. J. *J. Am. Chem. Soc.* **1993**, *115*, 6499–6505.
- (15) Vande Velde, C. M. L.; Geise, H. J.; Blockhuys, F. *Acta Crystallogr. C* **2005**, *61*, o21–o24.
- (16) Vande Velde, C. M. L.; Geise, H. J.; Blockhuys, F. *Cryst. Growth Des.* **2006**, *6*, 241–246.
- (17) *CAD-4 EXPRESS*; Enraf-Nonius: Delft, The Netherlands, 1989.
- (18) Harms, K.; Wocadlo, S. *XCAD4*; Universiteit Marburg: Duitsland, 1996.
- (19) *APEX2, SADABS and SAINT-Plus*; Bruker AXS Inc.: Madison, Wisconsin, USA, 2008.
- (20) Sheldrick, G. M. *Acta Crystallogr. A* **2008**, *64*, 112–22.
- (21) Spek, A. L. *J. Appl. Crystallogr.* **2003**, *36*, 7–13.
- (22) Macrae, C. F.; Bruno, I. J.; Chisholm, J. A.; Edgington, P. R.; McCabe, P.; Pidcock, E.; Rodriguez-Monge, L.; Taylor, R.; van de Streek, J.; Wood, P. A. *J. Appl. Crystallogr.* **2008**, *41*, 466–470.
- (23) Rohlíček, J.; Husák, M. *J. Appl. Crystallogr.* **2007**, *40*, 600–601.
- (24) Allen, F. H. *Acta Crystallogr. B* **2002**, *58*, 380–388.
- (25) Collas, A.; De Borger, R.; Amanova, T.; Blockhuys, F. *CrystEngComm* **2011**, *13*, 702–710.
- (26) Harada, J.; Harakawa, M.; Ogawa, K. *Acta Crystallogr. B* **2004**, *60*, 578–588.
- (27) Verbruggen, M.; Yang, Z.; Lenstra, A. T. H.; Geise, H. J. *Acta Crystallogr. C* **1988**, *44*, 2120–2123.
- (28) Vande Velde, C. M. L.; Chen, L. J.; Baeke, J. K.; Moens, M.; Dieltiens, P.; Geise, H. J.; Zeller, M.; Hunter, A. D.; Blockhuys, F. *Cryst. Growth Des.* **2004**, *4*, 823–830.
- (29) Vande Velde, C. M. L.; Baeke, J. K.; Geise, H. J.; Blockhuys, F. *Acta Crystallogr. C* **2005**, *61*, o284–o287.